Electronic Supporting Information

Intercalation-exfoliation processes during ionic exchange reaction from the sodium lepidocrocite-type titanate toward the proton-based trititanate structure

Seongkoo Kang,[a,b] Serge Durand-Vidal,[a,b]* Jean-Claude Badot,[b,c] Christophe Legein,[d] Monique Body,[d] Olaf J. Borkiewicz,[e] Olivier Dubrunfaut,[f] and Damien Dambournet[a,b]*

[a] *Sorbonne Université, CNRS, Physicochimie des Electrolytes et Nanosystèmes Interfaciaux, PHENIX, F-75005, Paris, France*

[b] *Réseau sur le Stockage Electrochimique de l'Energie (RS2E), FR CNRS 3459, 80039 Amiens ,France*

[c] *Chimie ParisTech, PSL Research University, CNRS, Institut de Recherche de Chimie Paris, 11 rue Pierre et Marie Curie, 75005 Paris, France*

[d] *Institut des Molécules et Matériaux du Mans (IMMM) - UMR 6283 CNRS, Le Mans Université, Avenue Olivier Messiaen, 72805 Le Mans Cedex 9, France*

[e] *X-ray Science Division, Advanced Photon Source, Argonne National Laboratory, Argonne, Illinois 60439, United States*

[f] *GeePs Group of Electrical Enginering – Paris, UMR CNRS 8507, CentraleSupélec, Sorbonne Université, Univ Paris-Sud, Université Paris-Saclay, 11 rue Joliot-Curie, 91192 Gif-sur Yvette, France*

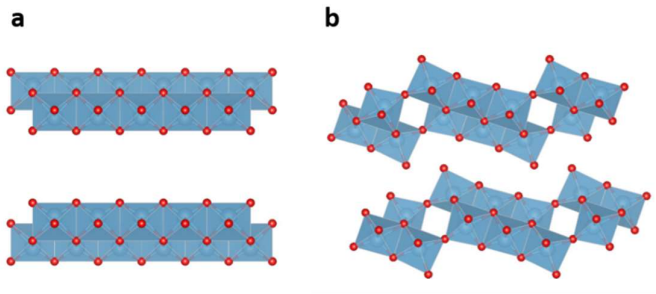

Fig. S1. Structural representation of a) lepidocrocite and b) trititanate structure.

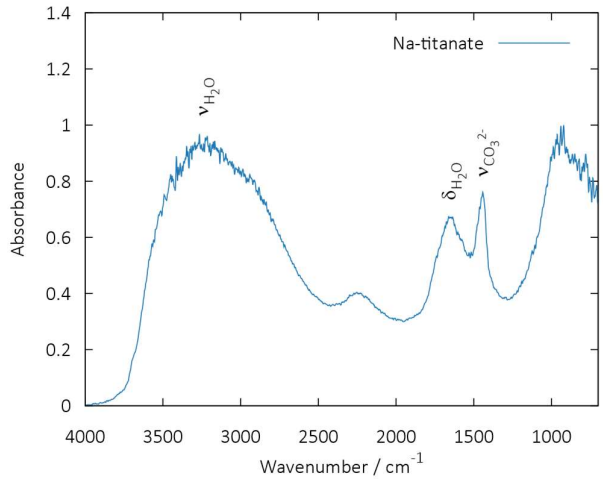

Fig. S2. ATR FT-IR spectrum of Na-titanate.

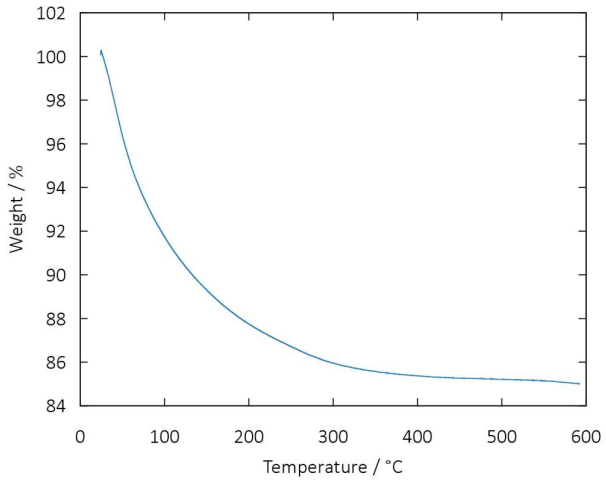

Fig. S3. Thermogravimetric analysis curve of Na-titanate.

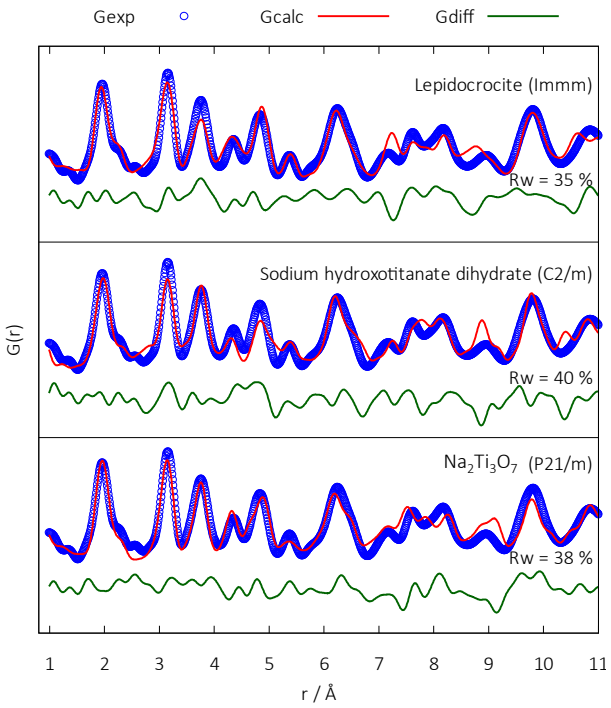

Fig. S4. PDF refinements of Na-titanate using different structural models.

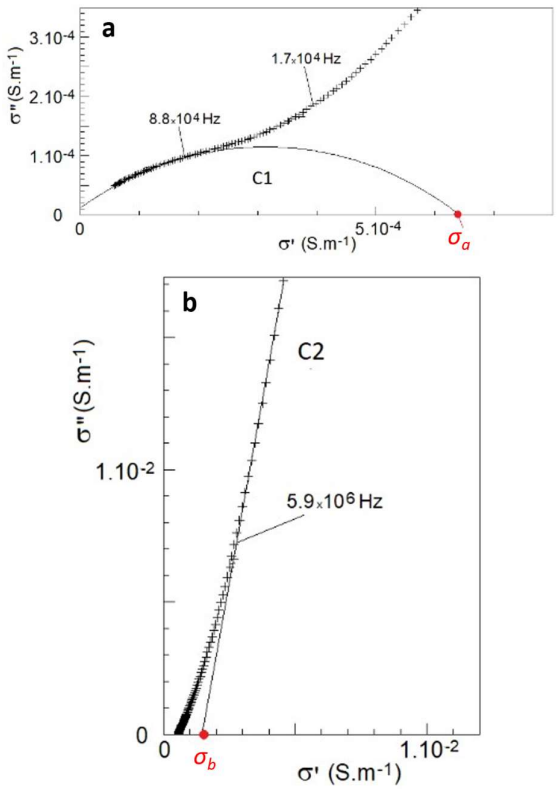

Fig. S5. Nyquist plots of conductivity at RT.
a) Low-frequency contribution (double layer capacitance) C1 fitted with a circular arc.
b) Grain bulk contribution fitted with a straight line obtained after the subtraction of C1.
σ_a = 6.4·10^{-4} S/m and σ_b = 1.5·10^{-3} S/m are sample and grain conductivities, respectively.

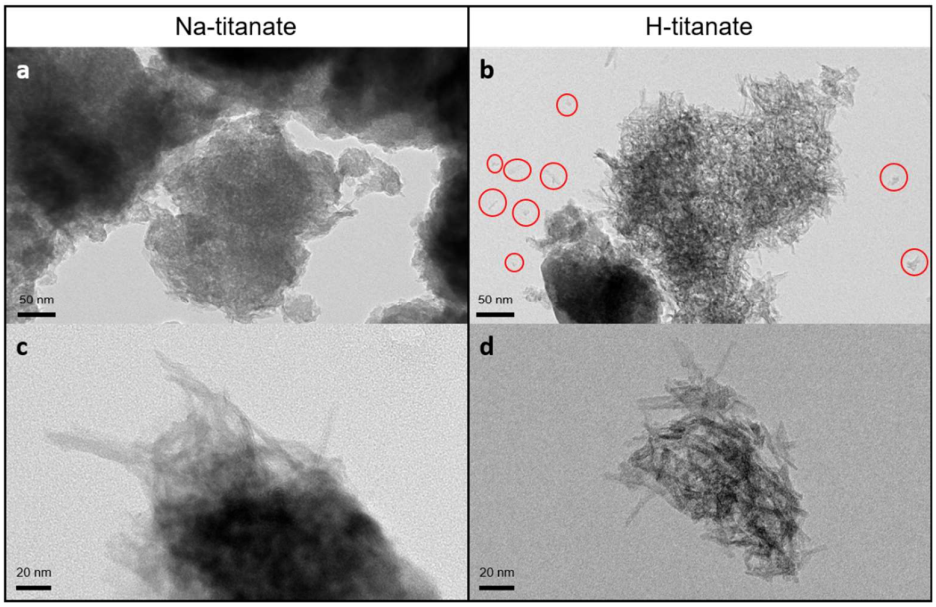

Fig. S6. TEM images of Na-titanate (a, c) and H-titanate (b, d).

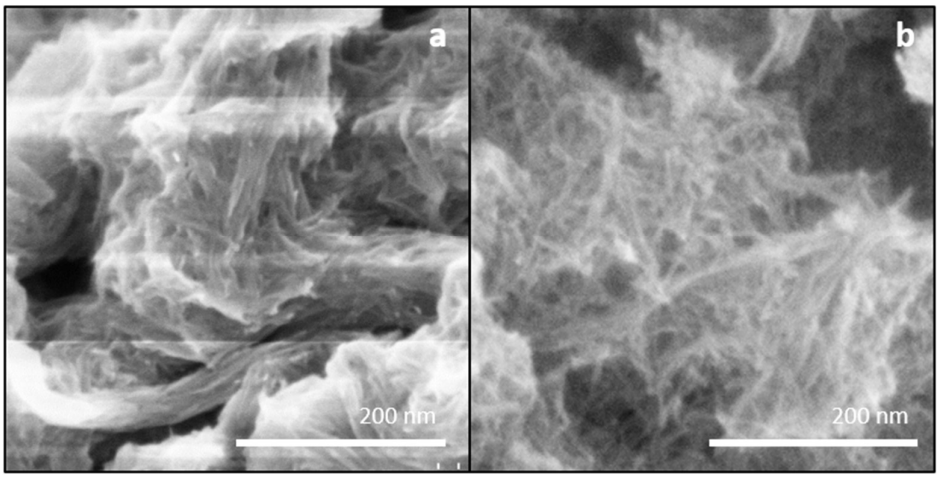

Fig. S7. SEM images of Na-titanate (a) and H-titanate (b)

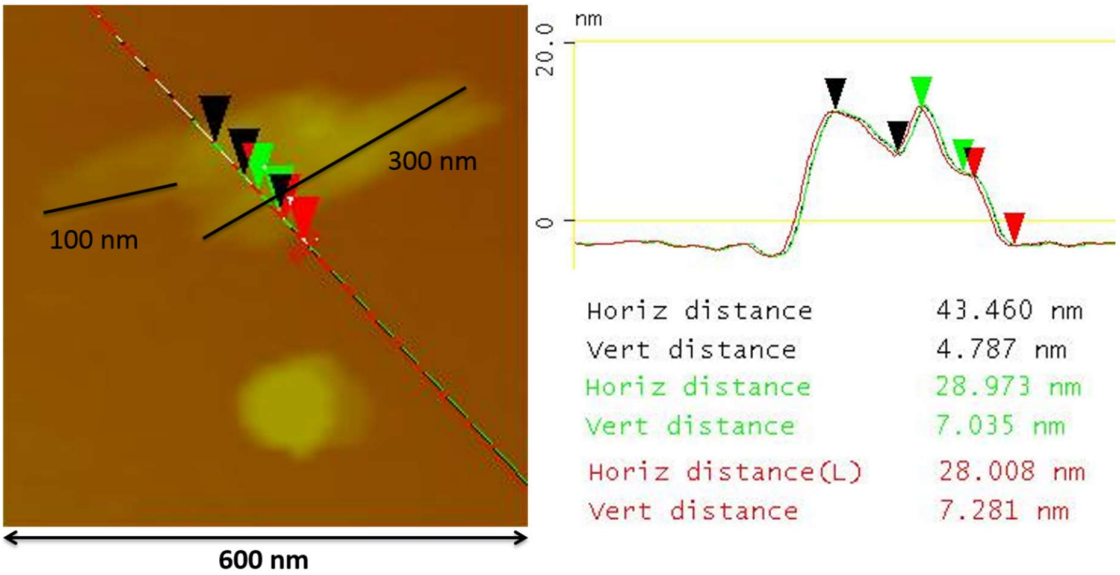

Fig. S8. Atomic force micrograph with a section of an aggregate of elongated particles of H-titanate. Horizontal and vertical distances are between black, green, and red arrows. The longest sizes of two elongated particles are given in the picture.

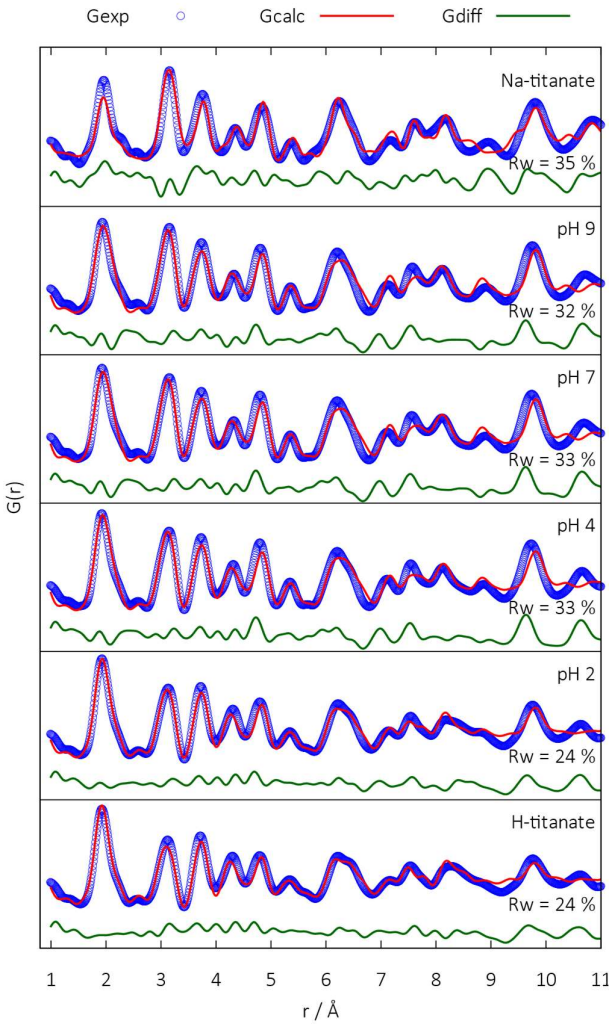

Fig. S9. Real-space refinements of the PDFs of the samples collected at different pH values.

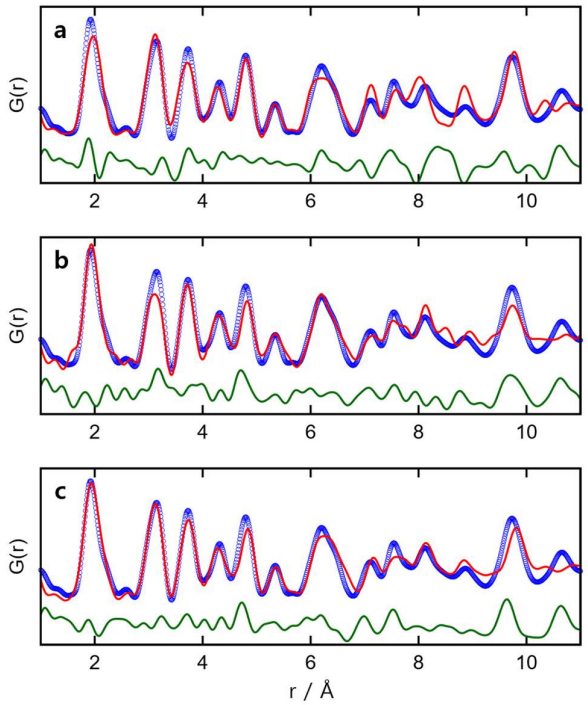

Fig. S10. Real-space refinements of the PDF of the sample collected at pH 4 using lepidocrocite (a), trititanate (b), and both models (c).

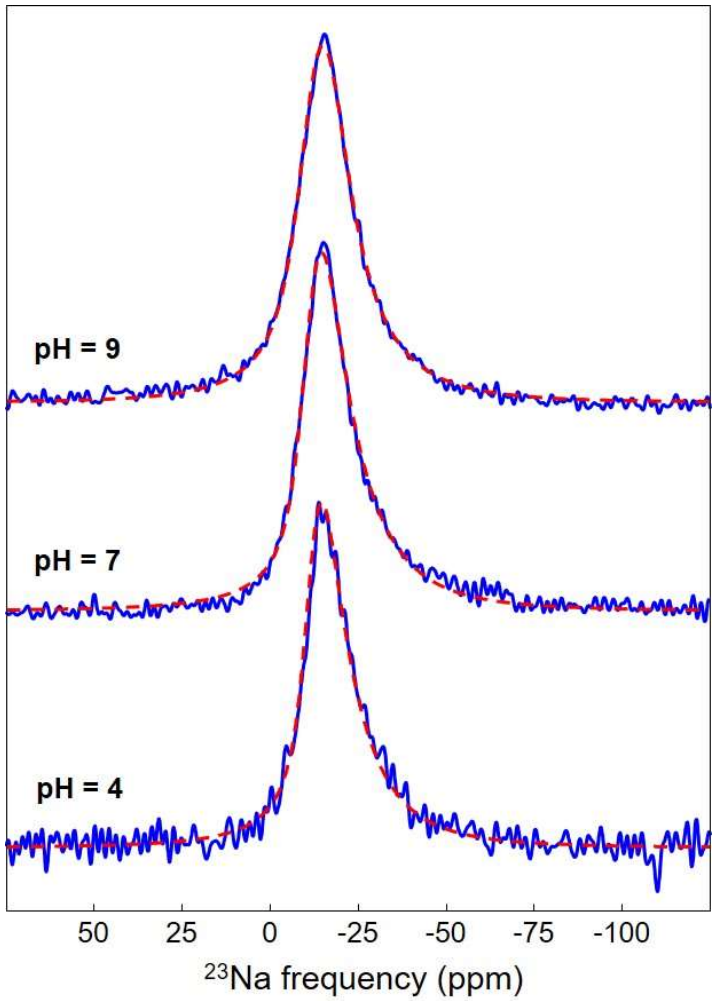

Fig. S11. Experimental (blue) and fitted using the Gaussian Isotropic Model[1] (red dashed line) ^{23}Na MAS (44 kHz) NMR spectra of three samples collected at different pH values. This model involves a Gaussian distribution of chemical shifts and a distribution of quadrupolar interactions. The parameters used for these fits are reported in **Table S1**.

Table S1. Average isotropic chemical shift (<δ_{iso}>/ppm), full width at half maximum (FWHM) of the isotropic chemical shift Gaussian distribution (ΔCS/ppm), average quadrupolar frequency (<ν_Q>/kHz) and quadrupolar constant (<C_Q>/MHz) used to fit the ^{23}Na MAS NMR spectra of three samples collected at different pH values (see **Fig. S8**).

pH	<δ_{iso}>	ΔCS	<ν_Q>	<C_Q>
9	-12.6	9.1	515	1.03
7	-11.3	7.0	668	1.34
4	-11.7	5.8	631	1.26

[1] D. Massiot, F. Fayon, M. Capron, I. King, S. Le Calvé, B. Alonso, J.-O. Durand, B. Bujoli, Z. Gan and G. Hoatson, Modelling one- and two-dimensional solid-state NMR spectra: Modelling 1D and 2D solid-state NMR spectra, *Magn. Reson. Chem.*, 2002, **40**, 70–76.

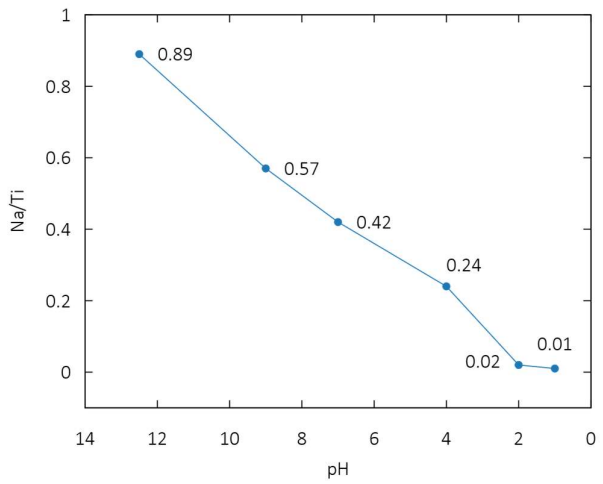

Fig. S12. Na/Ti ratio quantified using energy dispersive X-ray spectroscopy for the samples collected at different pH.

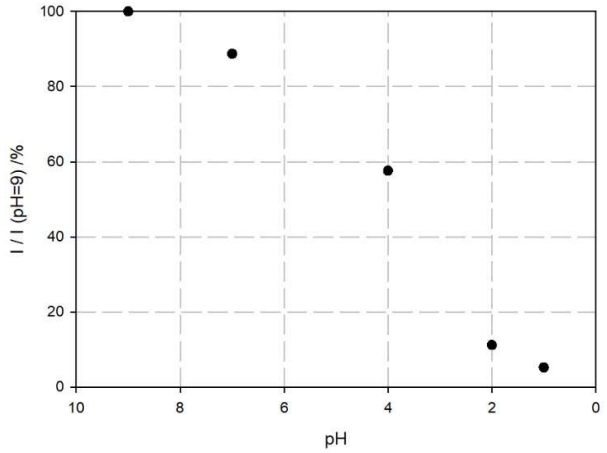

Fig. S13. Intensity / Intensity (pH = 9) ratio of the ^{23}Na non-normalized NMR spectra for the samples collected at different pH. Intensity estimated as the area under the curve of the fit of each non-normalized spectrum. The ^{23}Na non-normalized spectra correspond, for each sample, to the same number of scans and the same sample mass in the rotor.

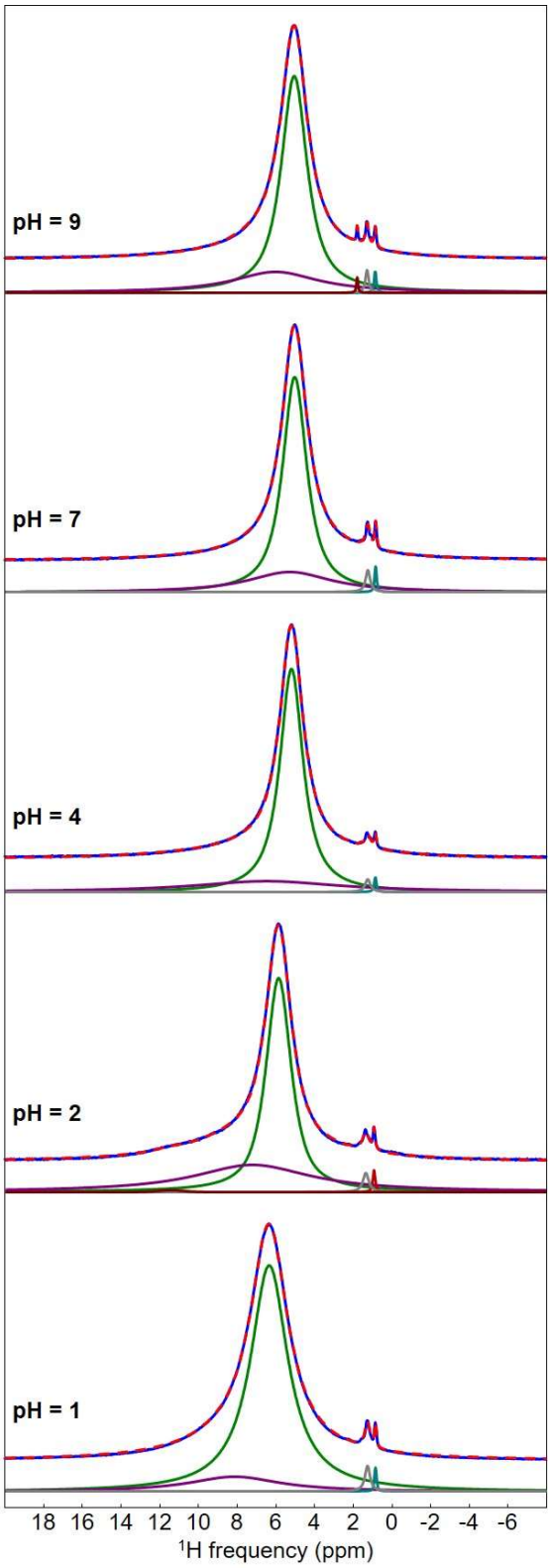

Fig. S14. Experimental (blue) and fitted (red dashed line) ^{1}H MAS (60 kHz) NMR spectra of the samples collected at different pH. The individual resonances used for these fits are shown below (see **Table S2**).

Table S2. Isotropic chemical shifts (δ_{iso}/ppm), line widths (LW/ppm), relative intensities (I/%), of the NMR resonances used for the fit of the ^{1}H MAS (64 kHz) NMR spectra of the samples collected at different pH (see **Fig. S11**).

pH	δ_{iso}	LW	I
1	0.85	0.13	0.4
	1.26	0.31	1.3
	6.3	2.3	84.9
	8.1	5.7	13.4
2	0.92	0.14	0.6
	1.35	0.36	1.3
	5.9	1.6	60.3
	7.2	7.3	37.5
	11.4	1.5	0.3
4	0.85	0.14	0.5
	1.25	0.34	1.0
	5.2	1.5	74.6
	6.5	9.1	23.9
7	0.84	0.12	0.7
	1.24	0.28	1.4
	5.0	1.5	73.5
	5.3	5.3	24.4
9	0.86	0.13	0.6
	1.28	0.20	1.0
	1.8	0.09	0.3
	5.1	1.6	74.5
	6.0	5.4	23.6

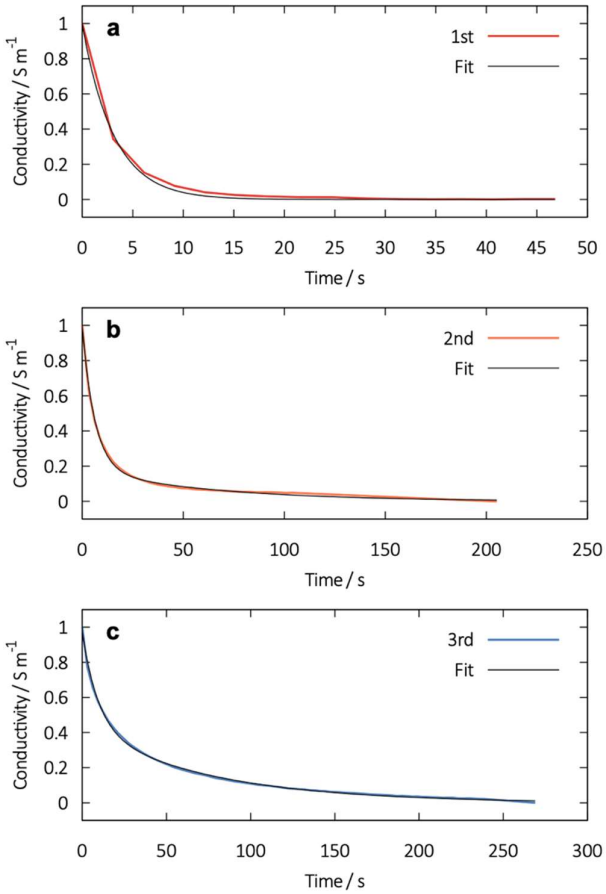

Fig. S15. Results of to fit the decay of the ionic conductivity during the Na^+-H^+ ionic exchange.